Thermal Imaging Fault Detection for Rolling Element Bearings

Abid Abdul Azeez
Mechanical Engineering Department
Abu Dhabi University
Abu Dhabi, UAE
abid.azeez@adu.ac.ae

Mohammad Alkhedher
Mechanical Engineering Department
Abu Dhabi University
Abu Dhabi, UAE
mohammad.alkhedher@adu.ac.ae

Mohamed S. Gadala
Mechanical Engineering Department
Abu Dhabi University
Abu Dhabi, UAE
mohamed.gadala@adu.ac.ae

***Abstract*—In rotating machinery, rolling element bearings are one of the most critical components and a large majority of system failures arise from faulty bearings. Hence, there is an increasing demand to find an effective and reliable condition monitoring technique. In this paper, a procedure for detecting various types of bearing faults using thermal imaging is presented and assessed. Five different fault cases are tested: no fault (NF), line fault (LF), small circle fault (SCF), double line fault (DLF), and large circle fault (LCF). Experiments were conducted on the BENTLY NEVADA RK4 Rotor Kit. The tests were performed at 1500 RPM and 2000 RPM. A video is recorded for 10 minutes using FLIR thermal imaging camera and images are extracted from the video and processed to detect the average temperature at the bearing hotspot using MATLAB. Analysis of the results show that Thermal Imaging can be used as an effective means to differentiate between different types of faults that occur in the outer race of the rolling element bearing.**

Keywords— Thermal Imaging Camera, Rolling Element Bearing, Fault Detection, Outer Race, Preventive Maintenance.

I. INTRODUCTION

IN recent years, condition monitoring and fault diagnosis of rotating equipment are of great concern in various industries. Early fault detection in machineries may save millions of dollars in emergency maintenance costs. In rotating machinery, rolling element bearings are one of the most critical components and a large majority of system failures arise from faulty bearings. Proper and reliable functioning of these machine elements is critical to prevent long term, costly catastrophic downtimes. A reliable online machinery condition monitoring system is valuable to a wide array of industries to recognize an incipient machinery defect so as to prevent machinery performance degradation, malfunctions, or even catastrophic failures [1]. Innovative and easy to implement techniques are needed to monitor the health status of bearings efficiently and effectively [2].

Rolling element bearings are machine elements that permit rotary motion of shafts and eliminate sliding friction in machinery for a wide range of applications such as turbines, pumps, compressors, power transmission, and motors, [3]. Compared to other types of bearings, rolling bearings have many advantages. They are often referred to as antifriction elements and they require small amount of lubrication [1]. Rolling bearings can reliably operate at high-speeds and can support considerable radial and axial loads.. A typical rolling element bearing consists of: an outer race, an inner race, rolling elements that are in contact under heavy dynamic loads and relatively high speeds, and a cage around these rolling elements to maintain spacing, as shown in Fig. 1

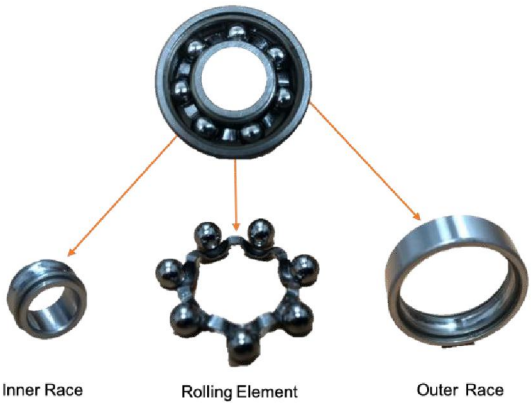

Fig. 1. Rolling Element Bearing Components

Faults may occur in any of these parts, and often these faults are single point defects such as chips or dents [4]. As these elements move relative to each other, these defects come into periodic contact with other elements in the bearing, and at each contact they can excite a high frequency resonance in the assembly. Rolling bearing damage may result in a complete failure of the bearing or reduction in the operating efficiency of the bearing arrangement. Only if operating and environmental conditions as well as the details of the bearing arrangement are completely in tune; the bearing arrangement operate efficiently. Bearing damage mostly initiate from the operating conditions and bearing defects in material or workmanship is exceptional [5].

Bearings are the common elements used in heavy rotating machinery and equipment because of their high reliability. Bearings start to malfunction due to machine overload, shaft misalignment, rotor unbalance, overheating, manufacturing defects, etc. Many different techniques have been developed to early detect and extract bearing fault features. These may be broadly classified as vibration measurements, acoustic measurements, temperature measurements and wear debris analysis. Vibration techniques are not sensitive to incipient faults and they are usually masked by background noise caused by mechanical vibration signals from rotating machinery. Hence, it is normally difficult for the vibration techniques to detect bearing faults at an early stage. Acoustic emission (AE) is the phenomenon of transient elastic wave generation due to a rapid release of strain energy caused by relative motion of small particles under mechanical stresses. The frequency content of acoustic emission (AE) is typically in the range of 100 kHz to 1 MHz, therefore AE is not

influenced or distorted by imbalance and misalignment which are at low frequency ranges. The high sensitivity of AE technique and its ability to detect the initial phase of component degradation has become one of the significant advantages of AE over vibration measurement. However, limitations in using AE technique for monitoring bearings have been partly due to the difficulty in processing, interpreting and classifying the acquired data, and the relatively more expensive setup. In this research, temperature measurement technique is applied with the use of thermal imaging camera.

II. Literature review

There are several modes of bearing failure which include fatigue damage, plastic deformation, common wear, damage due to corrosion, brinelling, inadequate lubrication, faulty installation, and incorrect design.

Damage due to fatigue initiates with the introduction of tiny cracks underneath the surface of the bearing. As the run continues, cracks develop to the surface and cause the material to break at contact points. Spalling, pitting or flaking of the rolling elements or bearing races can be found as a result of the actual failure. In case the bearing lingers during service, the damage would expand in the location of the defect due to the development of stress concentration. [6]

Common wear is another mode of bearing failure. Polluted lubricant or inadequate sealing of bearings may allow foreign particles or dirt to enter the bearing. These particles upon entry roughen the surfaces thereby producing a rough appearance. In the case of drastic wear, the raceway, rolling diameter, and element profile will change thereby increasing the bearing clearance. In such circumstances, the rolling friction becomes significant and may lead to high levels of slipping or skidding. This could result in complete breakdown of a machine. [6]

Plastic deformation is another mode of bearing failure where the contacting surfaces can be as a result of the bearing being subject to huge amounts of loads while undergoing small or stationary movements. This leads to indentation of the gutter since excessive loading results in plastic deformation at that particular location. Due to the deformation in the bearing, the bearing cannot be used further as it would produce a lot of vibration as it rotates unevenly. [6]

Corrosion damage is caused when there is the presence of acids, water or other contaminants in the oil that enters the bearing segment. The bearings are generally operated in high temperatures. Cooling down of bearing in very humid air can result in producing damaged seals, condensation or acidic lubricants. Noisy and uneven operation can be observed due to the presence of rust on the bearing surface. This is due to the rust particles that prevent the smooth rolling action and lubrication of the rolling elements. [7]

Brinelling is a defect that results in spaced indentations. These indentations are distributed over the entire raceway circumference of the rolling element bearing. There are three possible causes of brinelling: Plastic distortion of the raceways due to static overloading, A stationary rolling bearing is introduced to vibration and shock loads, and A bearing forms the loop for the passage of electric current. [7]

Inadequate lubrication is another mode of bearing failure. It leads to slipping, skidding, heat generation, sticking and increased friction. When there is deficiency of lubricant in the region of contact, the contacting surfaces rub together causing wear as the rolling element is moving. The three major points of bearing lubrication are the roller-race interface, the cage-race interface and the cage-roller interface. [7]

Faulty installation can result in undue preloading in either axial or radial directions, loose fit, misalignment or damage due to extreme force used in attaching the bearing components together. Incorrect design can result in underprivileged choosing of bearing size or type for a certain operation. It could also result in insufficient support by the coupling parts. Incorrect bearing selection can affect in numerous problems subject to whether it includes low load carrying competency or low speed rating. The end outcome is premature failure and fatigue life. [8]

Incorrect design can involve underprivileged choice of bearing size or type for the required operation, or insufficient support by the coupling parts. Incorrect bearing selection can affect in any number of problems subjected to whether it includes low load carrying competency or low speed rating. Once again, the end outcome will be reduced premature failure and fatigue life [8].

Bearing scattered defects may generate too much heat in the rotating components. Monitoring the temperature of a bearing lubricant or housing may be an efficient method for fault detection of rotary machines [9].

A multi-sensor system is implemented such that it uses vibration measurement data as well as infrared thermal imaging data for fault detection and diagnostics. The results show that by combining the data from multi-sensor system, a more accurate condition monitoring system is developed when compared with the results obtained using individual sensors. The disadvantage, however, is the financial cost that increases as two sensors are required. A cost-benefit analysis should be conducted prior to implementing a multi-sensor system. [10].

An automatic bearing fault diagnosis approach using non-invasive contactless thermal infrared imaging is proposed for early fault diagnosis of an induction motor. Thermal images of four different bearing conditions in a three phase induction motor: outer race defected bearing, inner race defected bearing, lack of lubrication and healthy bearing is analyzed. As a first step thermal images of induction motor were acquired then preprocessed using 2D-DWT to decompose the thermal images. This is followed by extracting relevant features and selecting the strongest feature using Mahanabolis distance critera. Finally the selected features are given to a SVM (Support Vector Machine) classifier for classification of bearing condition [11].

III. Experimental setup

The experimental setup consists of the GE Bentley Nevada RK4 Rotor Kit as shown in Fig 2. The kit includes a motor, coupling, drive assembly, drive belts, and two proximity probes for motor speed control and Keyphasor signal pickup.

The spindle can be driven up to 10,000 RPM.

A FLIR thermal camera (FLIR A615), not shown in figure, is used to capture thermal images and is connected to a laptop that runs the FLIR tools software for the thermal imaging camera. The specifications of the camera are listed in Table I.

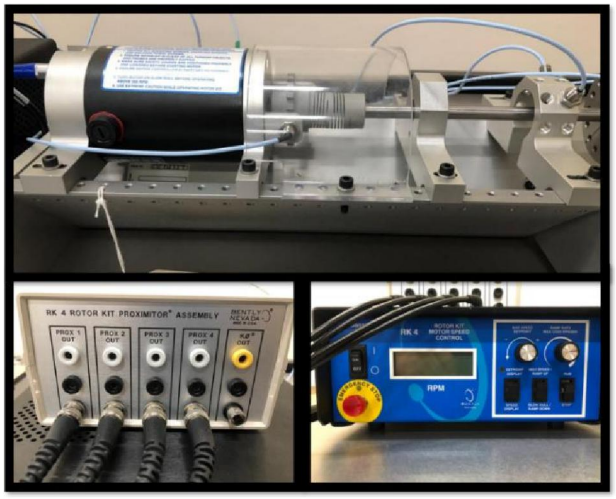

Fig. 2. GE Bently Nevada RK4 Rotor Kit

Bearing specification	SKF 6000-2RSH/C3
Ball diameter (d)	6 (mm)
Pitch diameter (p)	18 (mm)
Number of rollers (n)	7
Contact Angle (α)	0
Bearing specification	SKF 6000-2RSH/C3

TABLE I
Thermal Camera Specifications

Focal Length	41.3 mm
Housing Material	Aluminum
IR Resolution	640 x 480 pixels
Object Temperature Range	-20 to +150oC, +100 to +650oC, +300 to +2000oC
Operating Temperature Range	-15oC to +50oC
Emissivity Correction	Variable from 0.01 to 1.0
Camera Size	222 x 73 x 75 mm

TABLE II
Bearing Specifications

The rolling element bearing chosen for the experiment is SKF 6000-2RSH/C3 ball bearing. The specifications of the bearing are shown in Table II.

The schematic of the experimental setup that uses the thermal imaging camera is shown in Fig. 3. The thermal camera is placed at an angle and a distant such that the inner and outer race of the bearing are in the point of view.

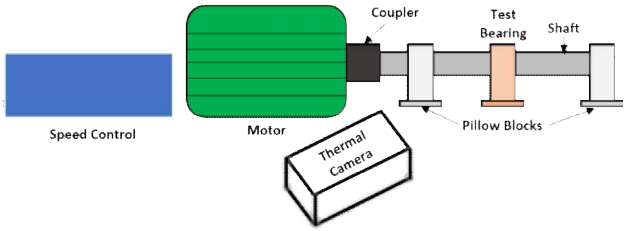

Fig. 3. Thermal Camera Schematic

IV. Methodology

The common techniques used to extract features from IR images include image averaging, image normalization, time derivative, peak contrast, central moments, standard deviation, mean, skewness, kurtosis, etc. However, the below method is employed to extract the features from the IR images.

The Thermal camera is set up in a position that is suitable to view the bearing. The resolution is set to 200 frames per second to achieve better accuracy in the results obtained. The Tests were conducted on a day to day basis in order to maintain the ambient temperature (Air condition was switched off) to avoid any errors in the data collected. The light in the room was also turned off in order to avoid any reflective temperature from the lights.

The emissivity value of 0.32 was inserted into the software since the inner and outer race of the bearing is made of mild steel. A video was recorded for 10 minutes of each case. Images were captured at intervals ranging 30 seconds from 0 – 10 minutes. The average temperature of the hotspot was obtained using MATLAB.

The tests conducted using the experimental setup include two cases; one with 1500 rpm and the second with 2000 rpm.

The tests are conducted five times each for the no fault, line fault (LF), small circle fault (SCL), double line fault (DLF), and large circle fault (LCF). The following steps have been followed to identify the faults as well as to differentiate between the types of faults.

A video of 10 minutes is captured for each of the test performed at both 1500 RPM as well as 2000 RPM. The video is later viewed using the FLIR tools software. Images are then captured at intervals of 30 seconds each from 0 to 10 minutes. A sample image captured using the software is shown in Fig. 4.

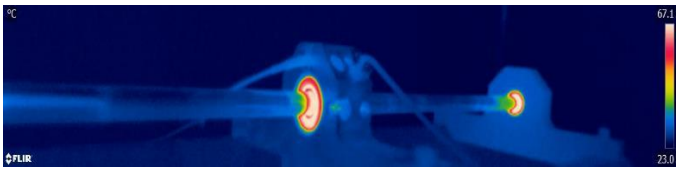

Fig. 4. Sample Thermal Image using FLIR tools

The images that are captured using the FLIR tools software are then imported to MATLAB to determine the average temperature at the hotspot using image processing techniques. The following procedure is followed to determine the average temperature at the hotspot:

a) An interface is created where the user is required to load the thermal image. The color map is then selected.

b) The analysis area is selected and the input parameters such as the maximum and minimum temperatures in the color map, and the temperature unit are to be entered.

c) The hotspot region is highlighted and the average temperature at the hotspot region is displayed on the top of the image. A sample image obtained upon following the procedure is shown in Fig. 5.

Fig. 5. Sample Result from MATLAB

V. RESULTS

The results obtained from the thermal imaging camera are discussed in this section. The tests were conducted at 1500 RPM and at 2000 RPM. The fault cases are No Fault (NF), Line Fault (LF), Small Circle Fault (SCF), Double Line Fault (DLF), and Large Circle Fault (LCF). Fig. 6 depicts the temperature readings obtained for all the fault cases at 1500 RPM.

The temperature shown are the average temperature at the hotspot at intervals of 30 seconds from 0 – 10 minutes. It can be seen that the LCF exhibited the largest average temperature among the 5 cases. The second largest temperature was shown by the DLF. The lowest average is exhibited by NF. The temperature is higher for SCF up to 4 minutes and then the temperature is higher for DLF for the remaining 6 minutes. It can also be noticed that the temperature is quiet constant after the 7.5 minutes mark. This is because the rate of heat transfer is almost the same as the maximum heat generated beyond this time. The maximum average temperature was 68ºC at 10 minutes for the LCF case followed by 64ºC at 10 minutes for the DLF case. The temperature trend for all cases is such that LCF>DLF>SCF>LF>NF. This indicates that the fault can be identified using thermal imaging by recording samples of various faults.

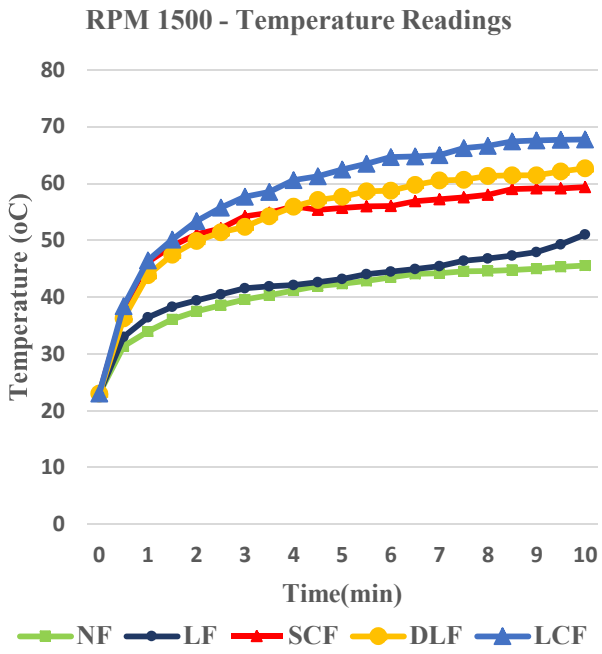

Fig. 6. Temperature Readings at 1500 RPM

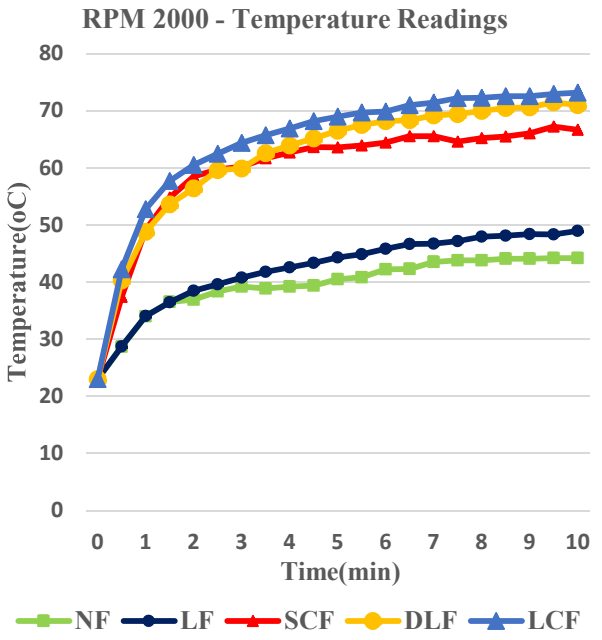

Fig. 7. Temperature Readings at 2000 RPM

Fig. 7 depicts the temperature readings obtained for all the fault cases at 2000 RPM. The temperature shown are the average temperature at the hotspot at intervals of 30 seconds from 0 – 10 minutes. It can be seen that the LCF exhibited the largest average temperature among the 5 cases. The second largest temperature was shown by the DLF. The lowest average is exhibited by NF. The temperature is higher for SCF up to 4 minutes and then the temperature is higher for DLF for the remaining 6 minutes. It can also be noticed that the temperature is quiet constant after the 7.5 minutes mark. This is because the rate of heat transfer is almost the same as the maximum heat generated beyond this time. The maximum average temperature was 74ºC at 10 minutes for

the LCF case followed by 72ºC at 9.5 minutes for the DLF case. The temperature trend for all cases is such that LCF>DLF>SCF>LF>NF. This clearly tells us that the fault can be identified using thermal imaging by recording samples of various faults.

VI. Conclusion

An experimental set up was used to record video using a thermal imaging camera to measure the temperature of the bearing. The data was acquired for a total of 5 cases at 2 different RPM. The cases are No Fault (NF), Line Fault (LF), Small Circle Fault (SCF), Double Line Fault (DLF), and Large Circle Fault (LCF). The RPM was set to 1500 and 2000. The video obtained from the camera is then processed using FLIR tools software to capture images at intervals of 30 seconds each from 0-10 minutes. The captured images were then processed in MATLAB to generate the average temperature of the hotspot region. From this research it was found that:

- Thermal Imaging can be used to different between different types of rolling element bearing faults that occur in the outer race of the bearing.
- The temperature varied for the different fault cases over the period of 10 minutes. The highest temperature was found in the Large Circle Fault (LCF). The second largest temperature was for the Double Line Fault (DLF) followed by the Small Circle Fault (SCF), and the Line Fault (LF).
- The graphs plotted for the various faults at different RPM indicate that bearing temperature can be used to differentiate between the types of faults.

The advantage of using thermal imaging camera is that a data acquisition or any other additional equipment is not required to extract and process the data. Traditional methods such as proximity probes, acoustic emission sensors, and other sensors require additional equipment such as pre-amplifier, proximitor assembly in addition to a data acquisition that is capable of handling huge sampling rates (2 million samples per second). Hence the use of thermal camera is also cost effective.

Further research and investigation in this area should be done on the following aspects:

- Analyzing a new test data for detecting multiple and extended faults on rolling element bearing components under different conditions.
- Conducting the experiment on a different set up and verifying the validity of the methodology implemented in this research
- Conducting more experiments using thermal camera to generate a database that will be sufficient to train a classifier.

References

[1] T. A. Harris, Rolling Bearing Analysis, 4th ed. ed., John Wiley & Sons Publication, 2001.

[2] G. Yadava, K. M. Ramakrishna, N. Tandon, "A comparison of some condition monitoring techniques for the detection of defect in induction motor ball bearings," Mechanical Systems and Signal Processing, vol. 21, pp. 244-256, 2007.

[3] V. Srinivasan, "Analysis of Dynamic Load Characteristics on Hydrostatic Bearing with Variable Viscosity and Temperature using Simulation Technique," Indian Journal of Science and Technology, vol. 6, 2013.

[4] P. D. McFadden, J. D. Smith, "The vibration monitoring of rolling element bearings by the high-frequency resonance technique - a review," Tribology International, vol. 17, no. 1, pp. 3-10, 1984.

[5] Z. Kiral, "Simulation And Analysis Of Vibration Signals Generated By Rolling Element Bearings With Defects," Ph. D. Thesis, 2002.

[6] S. A. Deshmukh and A. R. Askhedkar, "Survey of Fault Detection in Motor Ball Bearing," International Journal of Advanced Research in Electrical, Electronics and Instrumentation Engineering, vol. 6, no. 3, pp. 1329-1335, 2017.

[7] P. P. Kharche, R. D. Borole and M. P. Kharche, "Fault Detection in Rolling Element Bearing Using Vibration Based Analysis," in International Conference on Ideas, Impact and Innovation in Mechanical Engineering (ICIIIME 2017), 2017.

[8] Sorav Sharma, “Fault Identification in Roller Bearing using Vibration Signature Analysis”, Master’s Thesis, Department of Mechanical Engineering, Thapar University, Patiala, 2011.

[9] S. H. Ghafari, "A Fault Diagnosis System for Rotary Machinery Supported by Rolling Element Bearings," Canada, 2007.

[10] O. Janssens, M. Loccufier and S. V. Hoecke , "Thermal Imaging and Vibration-Based Multisensor Fault Detection for Rotating Machinery," IEEE Transactions on Industrial Informatics, vol. 15, no. 1, pp. 434-444, 2019.

[11] A. Choudhary, S. L. Shimi and A. Akula, "Bearing Fault Diagnosis of Induction Motor Using Thermal Imaging," in 2018 International Conference on Computing, Power and Communication Technologies (GUCON), Greater Noida, Uttar Pradesh, India, 2018.